Article

Modulated Conjugation as a Means of Improving the Intrinsic Hyperpolarizability

Javier Pe#rez-Moreno, Yuxia Zhao, Koen Clays, Mark G. Kuzyk, Yuquan Shen, Ling Qiu, Jumin Hao, and Kunpeng Guo

J. Am. Chem. Soc., **Article ASAP** • DOI: 10.1021/ja807394f • Publication Date (Web): 24 March 2009

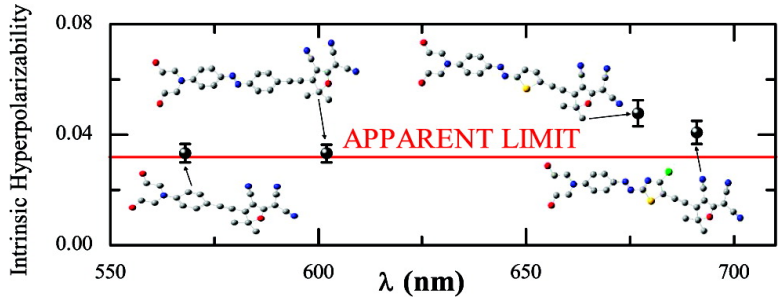

More About This Article

Additional resources and features associated with this article are available within the HTML version:

- Supporting Information
- Access to high resolution figures
- Links to articles and content related to this article
- Copyright permission to reproduce figures and/or text from this article

View the Full Text HTML

J|A|C|S
ARTICLES

Modulated Conjugation as a Means of Improving the Intrinsic Hyperpolarizability

Javier Pérez-Moreno,*[,†] Yuxia Zhao,[‡] Koen Clays,[†,§] Mark G. Kuzyk,[§] Yuquan Shen,[‡] Ling Qiu,[‡] Jumin Hao,[‡] and Kunpeng Guo[‡]

Department of Chemistry, University of Leuven, Celestijnenlaan 200D, B-3001 Leuven, Belgium, Technical Institute of Physics and Chemistry, Chinese Academy of Sciences, Beijing 100080, P. R. China, and Department of Physics and Astronomy, Washington State University, Pullman, Washington 99164-2814

Received September 18, 2008; E-mail: Javier.PerezMoreno@fys.kuleuven.be

Abstract: A new strategy for optimizing the first hyperpolarizability based on the concept of a modulated conjugated path in linear molecules is investigated. A series of seven novel chromophores with different types of conjugated paths were synthesized and characterized. Hyper-Rayleigh scattering experiments confirmed that modulated conjugation paths that include benzene, thiophene, and/or thiazole rings in combination with azo and/or ethenyl linkages between dihydroxyethylamino donor groups and various acceptor groups result in enhanced intrinsic hyperpolarizabilities that exceed the long-standing apparent limit for two of the chromophores. The experimental results are analyzed and interpreted in the context of quantum limits, which show that conjugation modulation of the bridge in donor/acceptor molecules simultaneously optimizes the transition moments and the energy-level spacing.

Introduction

Numerous applications in the field of second-order nonlinear optics, such as electro-optic modulation or frequency conversion require good nonlinear optical materials.[1] Applications generally require the nonlinear response time of such materials to be as short as possible. The optical nonlinearity of organic polymeric materials originates in the delocalized electronic cloud of the substituent molecules, which is known to have an ultrafast response. Most organic materials have a bulk nonlinear response that is related in a well-defined way to the molecular response; thus, researchers can focus on the optimization of the nonlinear molecular response of the building blocks used to make the bulk material. In this manner, the full richness of organic chemistry is available for the design and synthesis of efficient structures.[2−6]

In the search for large nonlinear molecular susceptibilities, considerable research effort has been expended toward optimization of the material parameters at the molecular level. This includes, among others, configuration locking in the all-trans configuration for a polyene bridge, shape optimization for reduced dipolar interaction, exploitation of coupled-oscillator physics, exploration of alternative noncentrosymmetric geometries, and, especially, optimization of the electron-donating and electron-withdrawing strengths of the terminal donor and acceptor groups, respectively.[4,7−13]

Surprisingly, the nature of the conjugation path *itself* has not been scrutinized to a similar extent. Except for reports on heteropentacyclic conjugation in second-order nonlinear optics and general rules based on the degree of aromaticity,[5,14−20] a more detailed study of the effect of the nature of the conjugation path has been lacking. There is a need for a more systematic

† University of Leuven.
‡ Chinese Academy of Sciences.
§ Washington State University.

(1) *Characterization Techniques and Tabulations for Organic Nonlinear Optical Materials*, 2nd ed.; Kuzyk, M. G., Dirk, C. W., Eds.; Marcel Dekker: New York, 1998.
(2) Singer, K. D.; Sohn, J. E.; King, L. A.; Gordon, H. M.; Katz, H. E.; Dirk, C. W. *J. Opt. Soc. Am. B* **1989**, *6*, 1339–1350.
(3) Teng, C. C.; Garito, A. F. *Phys. Rev. B* **1983**, *28*, 6766–6773.
(4) Cheng, L.-T.; Tam, W.; Stevenson, S. H.; Meredith, G. R.; Rikken, G.; Marder, S. R. *J. Phys. Chem.* **1991**, *95*, 10631–10643.
(5) Cheng, L. T.; Tam, W.; Marder, S. R.; Stiegman, A. E.; Rikken, G.; Spangler, C. W. *J. Phys. Chem.* **1991**, *95*, 10643–10652.
(6) Teng, C. C.; Garito, A. F. *Phys. Rev. Lett.* **1983**, *50*, 350–352.
(7) Shi, Y.; Zhang, C.; Zhang, H.; Bechtel, J. H.; Dalton, L. R.; Robinson, B. H.; Steier, W. H. *Science* **2000**, *288*, 119–122.
(8) Liu, S.; Haller, M. A.; Ma, H.; Dalton, L. R.; Jang, S.-H.; Jen, A. K.-Y. *Adv. Mater.* **2003**, *15*, 603–607.
(9) Dalton, L. R. *Synth. Met.* **2001**, *124*, 3–7.
(10) (a) Dalton, L. R. In *Electrical and Optical Polymeric Systems: Fundamentals, Methods and Applications*; Wise, D., Cooper, T., Gresser, J., Trantolo, D., Wnek, G., Eds.; World Scientific: Singapore, 1998; pp 609−662.
(11) Raimundo, J. M.; Blanchard, P.; Ledoux-Rak, I.; Hierle, R.; Michaux, L.; Roncali, J. *Chem. Commun.* **2000**, 1597–1598.
(12) Zyss, J.; Ledoux, I. *Chem. Rev.* **1994**, *94*, 77–105.
(13) Uyeda, H. T.; Zhao, Y.; Wostyn, K.; Asselberghs, I.; Clays, K.; Persoons, A.; Therien, M. J. *J. Am. Chem. Soc.* **2002**, *124*, 13806–13813.
(14) Mandal, K.; Kar, T.; Nandi, P. K.; Bhattacharyya, S. P. *Chem. Phys. Lett.* **2003**, *376*, 116–124.
(15) Pauley, M. A.; Wang, C. H. *Rev. Sci. Instrum.* **1999**, *70*, 1277.
(16) Jen, A. K.-Y.; Rao, V. P.; Wong, K. Y.; Drost, K. J. *J. Chem. Soc., Chem. Commun.* **1993**, 1118–1120.
(17) Robinson, B. H.; et al. *Chem. Phys.* **1999**, *245*, 35–50.
(18) Breitung, E. M.; Shu, C. F.; McMahon, R. J. *J. Am. Chem. Soc.* **2000**, *122*, 1154–1160.
(19) Malaun, M.; Kowallick, R.; McDonagh, A. M.; Marcaccio, M.; Paul, R. L.; Asselberghs, I.; Clays, K.; Persoons, A.; Bildstein, B.; Fiorini, C.; Nunzi, J.-M.; Ward, M. D.; McCleverty, J. A. *J. Chem. Soc., Dalton Trans.* **2001**, 3025–3038.
(20) Malaun, M.; Reeves, Z. R.; Paul, R. L.; Jeffery, J. C.; McCleverty, J. A.; Ward, M. D.; Asselberghs, I.; Clays, K.; Persoons, A. *Chem. Commun.* **2001**, 49–50.

10.1021/ja807394f CCC: $40.75

study of the importance of the conjugated spacer. In fact, recent theoretical work has suggested that one way to optimize the first hyperpolarizability is to generate a potential energy function that oscillates in a way that localizes the eigenfunctions on different parts of the molecule.[21] This type of oscillation can be realized in a molecule by varying the degree of conjugation of the bridge that separates the donor and acceptor ends of a chromophore. The oscillation of the potential energy function is implemented by taking advantage of the well-known difference in the aromatic stabilization energies of benzene and heteropentacyclics, such as thiophene rings.[5]

To systematically investigate this approach, we synthesized a series of molecules with a number of different conjugation paths, incorporating azobenzene, thiophene, and/or thiazole rings as well as azo and/or ethenyl bridges. The compounds were then characterized with hyper-Rayleigh scattering and the results analyzed with the aim of performing a more systematic study of the influence of the conjugation path. However, to achieve meaningful conclusions, it was necessary to differentiate between the effects of the molecular design and other factors that result in an enhancement of the first hyperpolarizability, such as the number of electrons and the size of the molecule. Such scaling issues were taken into account by comparing the intrinsic first hyperpolarizabilities,[22] which relate directly to the nonlinear efficiency of structures.[23]

Materials

For the (later) purpose of covalent incorporation of the chromophores in a polyurethane polymer at high loading levels,[24] all of the chromophores **1**−**7** have the dihydroxyethylamino electron-donor moiety (see Figure 1). The diol function allows each chromophore to be covalently linked in the polymer chain via its donor end only. This allows for a free choice of electron-acceptor groups. Chromophore **1** has the classical (di)nitro group in conjunction with a simple azo bridge. All of the other chromophores **2**−**7** have better acceptor groups: 2-dicyanomethylene-3-cyano-4,5,5-trimethyl-2,5-dihydrofuran (TCF) in **3**, **4**, **6**, and **7** and 3-phenyl-2-isoxazolin-5-one (PIO) in **2** and **5**.

p-Aminobenzaldehyde (Fluka), *N*,*N*-dihydroxyethylaniline (Aldrich), PIO (Aldrich), and *N*,*N*-dimethylaniline (Aldrich) were purchased and used without further purification. TCF, 2-amino-4-chloro-5-formylthiazole, and 1-(*N*,*N*-dihydroxyethyl)-4-formylaniline were prepared according to methods described in the literature.[25,26]

Chromophore **1** was synthesized according to a similar procedure described in our previous work.[27] Details of the syntheses of chromophores **1**−**6** have been published elsewhere.[28a]

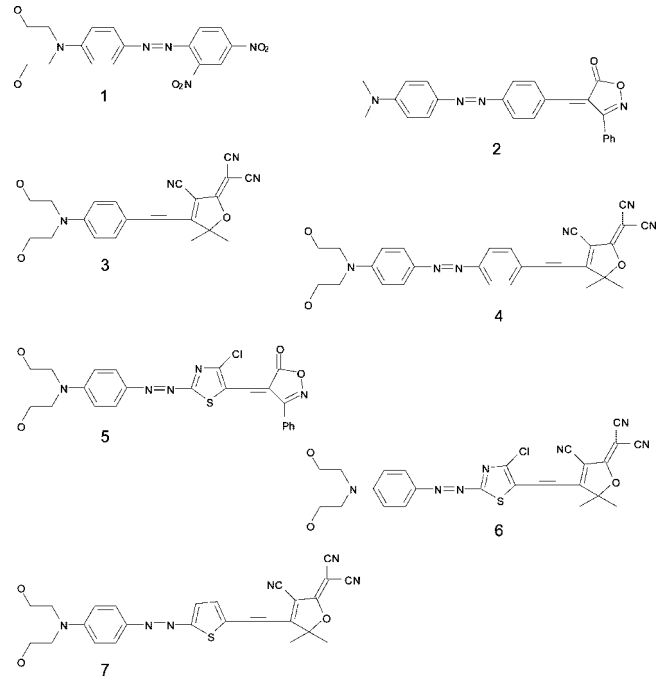

Figure 1. Chemical structures of the chromophores used in our study.

4-*N*,*N*-Dihydroxyethylamino-4′-formylazobenzene (b). Sodium nitrite (1.00 g, 14.5 mmol) was added in portions to 35 mL of cold sulfuric acid, and the mixture was warmed gradually to 70 °C (Figure 2). After all of the sodium nitrite was dissolved, the mixture was cooled to 5 °C. Next, 1.75 g (14.5 mmol) of 4-aminobenzaldehyde was added to the solution. The mixture was stirred for 2 h at 5−10 °C and then poured into 150 g of ice-cold water. After filtration, the diazonium solution was added dropwise to a solution of *N*,*N*-dihydroxyethylaniline in 30 mL of 0.1 N hydrochloric acid while maintaining the temperature at 10−15 °C. Next, 2 g of sodium acetate was added, after which the mixture was stirred at 10−15 °C for 2 h. The precipitate was collected, washed with water, and dried; the orange product (2.3 g) was used without further purification. Pure product could be obtained by column chromatography on silica gel with 3:1 petroleum ether/ethyl acetate as the eluent. IR (KBr, cm^{-1}): 3240 (−OH), 1690 (C═O), 1598 (N═N). λ_{max} (acetone): 450 nm.

4-*N*,*N*-Dimethylamino-4′-formylazobenzene (a). This compound was synthesized by a procedure similar to that for **b** (Figure 2). Yield: 68%. IR (KBr, cm^{-1}): 1659 (C═O), 1595 (N═N). UV−vis λ_{max} (nm): 447 (acetone).

Chromophore 2. A mixture of **a** (0.60 g, 2.37 mmol), PIO (0.39 g, 2.42 mmol), ammonium acetate (20 mg, 0.26 mmol), and acetic acid (30 mg, 0.5 mmol) in 25 mL of toluene was stirred for 4 h at 90 °C (Figure 2) and then cooled to room temperature. The precipitate was collected, washed with ethanol, and then recrystallized from ethanol to afford 0.61 g (64%) of pure product. IR (KBr, cm^{-1}): 3433, 1746, 1604, 1133. ^{1}H NMR (100 MHz, CD_3COCD_3): δ 8.58(d, 2H, J = 2.6 Hz), 7.92 (s, 1H), 7.88 (d, 4H, J = 2.6 Hz), 7.72 (d, 2H, J = 0.6 Hz), 7.64 (d, 2H, J = 0.6 Hz), 7.33 (m, 1H), 6.86 (d, 2H, J = 2.7 Hz), 3.13 (s, 6H). MS *m*/*z*: 396 (M^+), 264 [$M^+ - (CH_3)_2NC_6H_4N + 2H$].

Chromophore 4. A mixture of 0.92 g (2.9 mmol) of **b**, 0.60 g (3.0 mmol) of TCF, and 0.4 mL of 1:3 (v/v) piperidine/acetic acid in 20 mL of ethanol was refluxed for 4 h (Figure 2). The precipitate obtained was collected and washed with hot ethanol, and 0.8 g of product was obtained. The product was further purified by chromatography on silica gel with 5:1 chloroform/ethanol as the eluent. IR (KBr, cm^{-1}): 3423, 2229, 1600, 1132. ^{1}H NMR (100 MHz, CD_3COCD_3): δ 8.08 (d, 1H, J = 6.0 Hz), 8.03 (d, 2H, J = 3.0 Hz), 7.89 (d, 2H, J = 2.8 Hz), 7.83 (d, 2H, J = 2.8 Hz), 7.36 (d,

(21) Zhou, J.; Kuzyk, M. G.; Watkins, D. S. *Opt. Lett.* **2006**, *31*, 2891–2893.
(22) Zhou, J.; Kuzyk, M. G. *J. Phys. Chem.* **2008**, *112*, 7978–7982.
(23) Pérez-Moreno, J.; Zhao, Y.; Clays, K.; Kuzyk, M. G. *Opt. Lett.* **2007**, *32*, 59–61.
(24) Shen, Y.; Hao, J.; Qiu, L.; Cao, Z.; Yang, Y.; Shen, Q.; Clays, K.; Zhao, Y.; Persoons, A. *J. Nonlinear Opt. Phys. Mater.* **2004**, *13*, 55–63.
(25) Mellikian, G.; Rouessac, F. P.; Alexandre, C. *Synth. Commun.* **1995**, *25*, 3045–3051.
(26) Wang, J. H.; Zhou, J. Y.; Zhang, X. X.; Zhai, J. F.; Li, Z.; Shen, Y. Q.; Xu, G. *Chem. J. Chin. Univ.* **1999**, *20*, 237–242.
(27) (a) Qiu, L.; Zhang, J. X.; Zhai, J. F.; Shen, Y. Q. *Polym. J.* **1996**, *28*, 1027–1032. (b) Shen, Y. Q.; Qiu, L.; Li, Z.; Zhang, X. X.; Zhao, Y.; Zhai, J. F.; Delaire, J. A.; Nakatani, K.; Atassi, Y. *J. Mater. Sci.* **1999**, *34*, 1513–1517.
(28) (a) Qiu, L.; Shen, Y.; Hao, J.; Zhai, J.; Zu, F.; Zhang, T.; Zhao, Y.; Clays, K.; Persoons, A. *J. Mater. Sci.* **2004**, *39*, 2335–2340. (b) Hao, J.; Han, M.-J.; Guo, K.; Zhao, Y.; Qiu, L.; Shen, Y.; Meng, X. *Mater. Lett.* **2008**, *62*, 973–976.

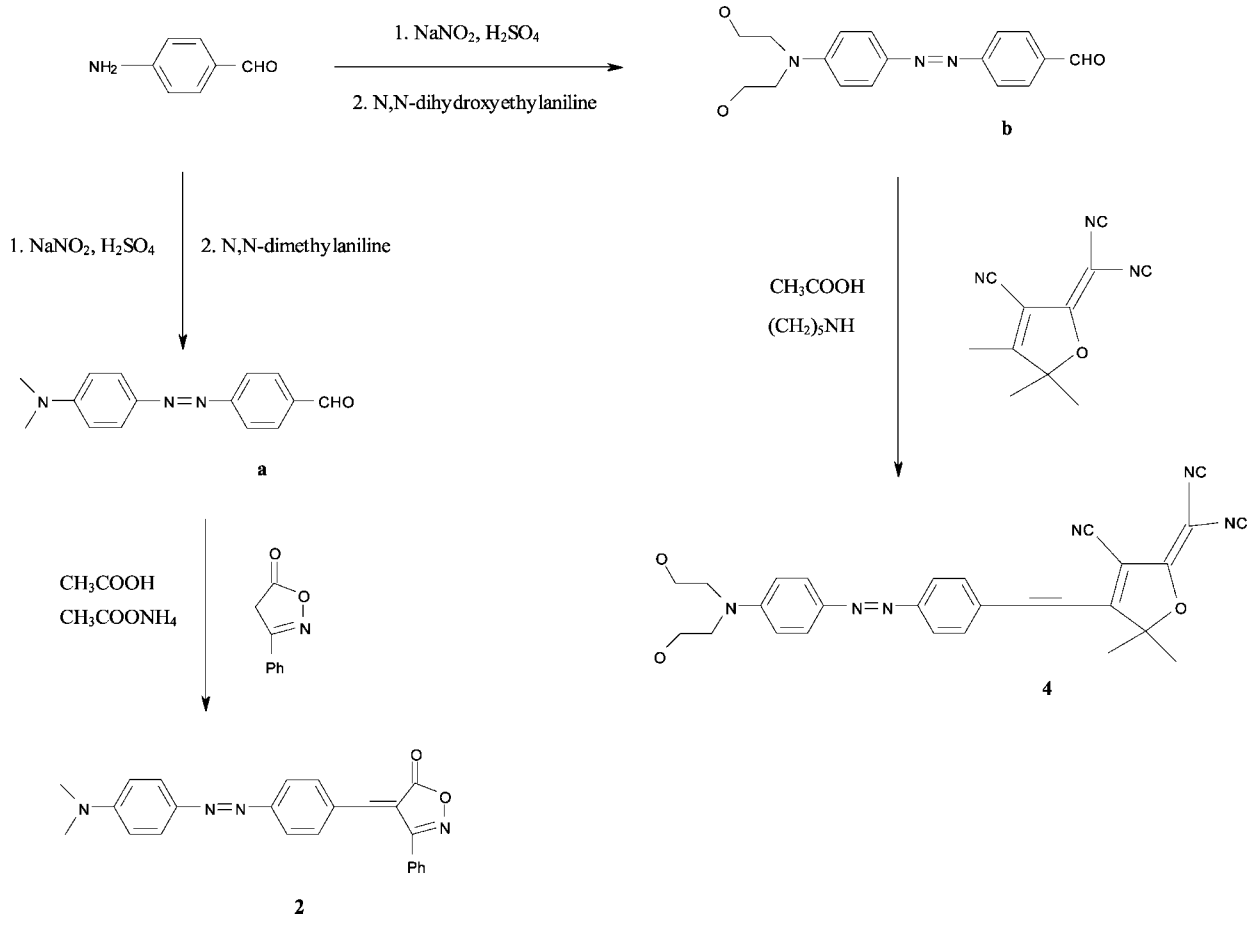

Figure 2. Chemical syntheses of chromophores **2** and **4**.

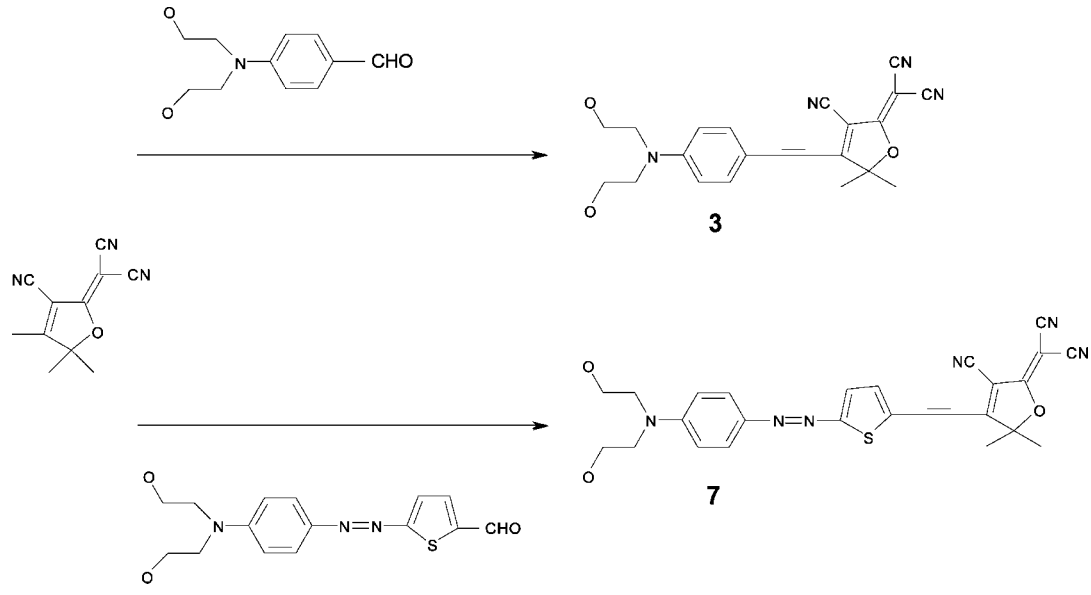

Figure 3. Chemical syntheses of chromophores **3** and **7**.

1H, $J = 6.0$ Hz), 6.92 (d, 2H, $J = 3.0$ Hz), 3.79 (t, 4H, $J = 1.0$ Hz), 3.70 (t, 4H, $J = 1.0$ Hz), 3.35 (s, 2H), 1.91 (s, 6H). MS *m/z*: 494 (M^+), 302 [$M^+ - (HOCH_2CH_2)_2NC_6H_4N + 2H$].

Chromophore 3. Piperidine (3 drops) was added to a mixture of 0.21 g (1.0 mmol) of 1-(*N*,*N*-dihydroxylethyl)-4-formylaniline and 0.230 g (1.1 mmol) of TCF in 6 mL of ethanol (Figure 3). The mixture was refluxed for 3 h and then cooled to room temperature. The solid was collected, washed with cool ethanol, and recrystallized from ethanol twice to afford 0.25 g of shiny blue-black crystals (65%). The product was further purified by chromatography on a silica column with 1:3 petroleum ether/ethyl acetate as the eluent. IR (KBr, cm^{-1}): 3425, 2975, 2978, 2848, 2228(−CN). ^1H NMR (100 GHz, DMF-d_7): δ 5.02 (t, 2H), 3.75 (s, 8H), 6.9−7.9 (m, 4H), 7.5 (d, 2H), 1.85 (s, 6H). MS *m/z*: 390 (M^+), 372 ($M^+ - H_2O$).

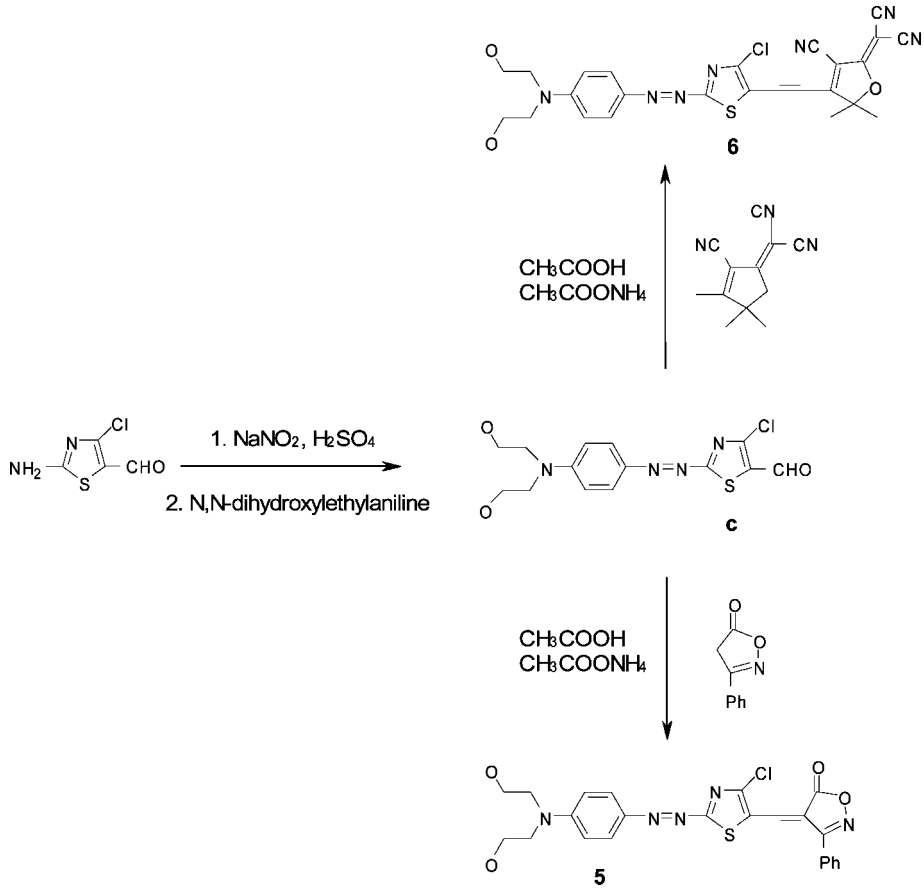

Figure 4. Chemical syntheses of chromophores **5** and **6**.

2-Formyl-5-(4′-*N*,*N*-dihydroxyethylaminophenylazo)thiophene (d). Details of this synthesis have been published elsewhere.[28b] IR (KBr, cm^{-1}): 3369, 3103, 2857−2963,1665. UV−vis λ_{max} (nm): 533.5 (DMF).

Chromophore 7. A mixture of 0.1 g (0.31 mmol) of **d**, 0.1 g (0.50 mmol) of TCF, a catalytic quantity of ammonium acetate, and several drops of acetic acid in 20 mL of ethanol was refluxed for 2 h (Figure 3) and then cooled to room temperature. The precipitate was collected, washed thoroughly with ethanol until the color of the filtrate became blue-green, and dried; the pure product was obtained in 90% yield. The product was further purified by chromatography on silica gel with 1:5 petroleum ether/ethyl acetate as the eluent. IR (KBr, cm^{-1}): 3423, 3090, 2870−2958, 2229. UV−vis λ_{max} (nm): 662 (DMF), 645.5 ($CHCl_3$). MS (TOF): 500.0 (M^+), 522 ($M^+ + Na - H$), 538 ($M^+ + K - H$).

Compound c. Sodium nitrite (1.5 g, 0.022 mol) was added in portions to 15 mL of cold sulfuric acid, and the mixture was warmed gradually to 70 °C (Figure 4). After all of the sodium nitrite was dissolved, the mixture was cooled to 5 °C and diluted with 10 mL of 1:4 (v/v) propionic acid/acetic acid. Next, 3.5 g (0.022 mol) of 2-amino-4-chloro-5-formylthiazole was added in portions to the solution at 5 °C, and the mixture was stirred at 5 °C for 30 min. The diazonium solution was then added dropwise to 4.1 g (0.023 mol) of *N*,*N*-dihydroxylethylaniline in 4.5 mL of sulfuric acid and 200 mL water at 0−5 °C. Sodium acetate (2 g) was added, after which the mixture was stirred at 0−5 °C for 1 h. The precipitate was collected, washed with water, and dried. The obtained product (1.5 g) was used directly in the following steps; it could be further purified by chromatography on silica gel with 1:1 petroleum ether/ethyl acetate as the eluent. IR: (KBr, cm^{-1}): 3237 (−OH), 1667 (C═O), 1599 (N═N). UV−vis λ_{max} (nm): 568 (acetone).

Chromophore 5. The synthesis of this chromophore was similar to the one for chromophore **2**, with **a** being replaced by **c** (Figure 4).

Chromophore 6. A mixture of 1.3 g (3.7 mmol) of **c**, 1.0 g (5.0 mmol) of TCF, 33 mg of ammonium acetate, and 50 mg of acetic acid in 40 mL of ethanol was refluxed for 2 h (Figure 4). The precipitate was collected and washed thoroughly with hot ethanol until the color of the filtrate changed from violet to blue. Drying yielded the pure product in 90% yield. The product could be further purified by chromatography on silica gel with 1:4 petroleum ether/ethyl acetate as the eluent. IR (KBr, cm^{-1}): 3433, 2228, 1603, 1133. ^1H NMR (100 MHz, CD_3SOCD_3): δ 8.05 (m, 1H), 7.77 (d, 2H, J = 2.4 Hz), 7.07 (d, 2H, J = 2.4 Hz), 6.88 (m, 1H), 3.70 (t, 4H, J = 0.5 Hz), 3.67 (t, 4H, J = 0.5 Hz), 3.36 (s, 2H), 1.17 (s, 6H). MS *m*/*z*: 535 (M^+), 343 [$M^+ - (HOCH_2CH_2)_2NC_6H_4N + 2H$].

Experiments

For chemical analysis, the standard measurements were performed. Mass spectra were recorded with a Trio-2000 spectrometer. ^1H NMR spectra were obtained with a Varian Gemini-300 spectrometer. Thermogravimetric analysis data were obtained using a Universal V2.5H TA instrument at a heating rate of 10 °C/min under N_2. The linear optical properties were also determined with commercial instrumentation. FTIR spectra were taken with a Bio-Rad FTS165 spectrometer. UV−vis spectra were determined on a UV-2001 spectrometer.

Analysis of Linear Absorption. The linear absorption spectrum of each sample was converted to molar extinction, ε (in units of M^{-1} cm^{-1}) using the Beer−Lambert law. The molar extinction spectra of the series of chromophores as a function of photon energy are shown in Figure 5.

From the first peak in the molar extinction spectrum, the energy difference between the ground and first excited states (E_{10}) is easily obtained. When the first peak in the molar extinction spectrum can be distinguished from the other peaks, the area under the peak can be related to the (dressed) first oscillator strength, yielding[29,30]

$$|\mu_{10}^*|^2 = \left(\frac{9.13 \times 10^{-3}}{E_{10}}\right)\int_0^\infty \varepsilon(E)\,\mathrm{d}E \tag{1}$$

where $\varepsilon(E)$ is the molar extinction (in units of M^{-1} cm^{-1}) as a function of the photon energy $E = \hbar\omega$ (in units of eV) and $|\mu_{10}^*|$ is the dressed transition dipole moment between the ground and first excited states. This result is obtained from the quantum-mechanical expression for the linear molecular polarization derived with perturbation theory[31] and assumes that the natural decay width is well-represented by a Lorentzian peak (with complex energy denominators). With the same units as in eq 1, the molar extinction as a function of the photon energy can be expressed as

$$\varepsilon(E) = 34.9\Gamma|\mu_{10}^*|^2\left[\frac{E}{(E_{10}-E)^2+\Gamma^2} - \frac{E}{(E_{10}+E)^2+\Gamma^2}\right] \tag{2}$$

where Γ is the line width of the first excited state, which can be estimated from the value of the maximum extinction at the peak, ε_{max}:

$$\Gamma \approx \frac{\int_0^\infty \varepsilon(E)\,\mathrm{d}E}{\pi\varepsilon_{max}} \tag{3}$$

To avoid overestimating the area under the first peak by direct integration, the values of the molar extinction were fitted to a log-normal function.[32] Table 1 lists the values of the parameters E_{10}, $|\mu_{10}^*|$, and Γ obtained from analysis of the first peak in the extinction spectrum.

To check the consistency of our method, we used the experimental values to plot the molar extinction as a function of photon

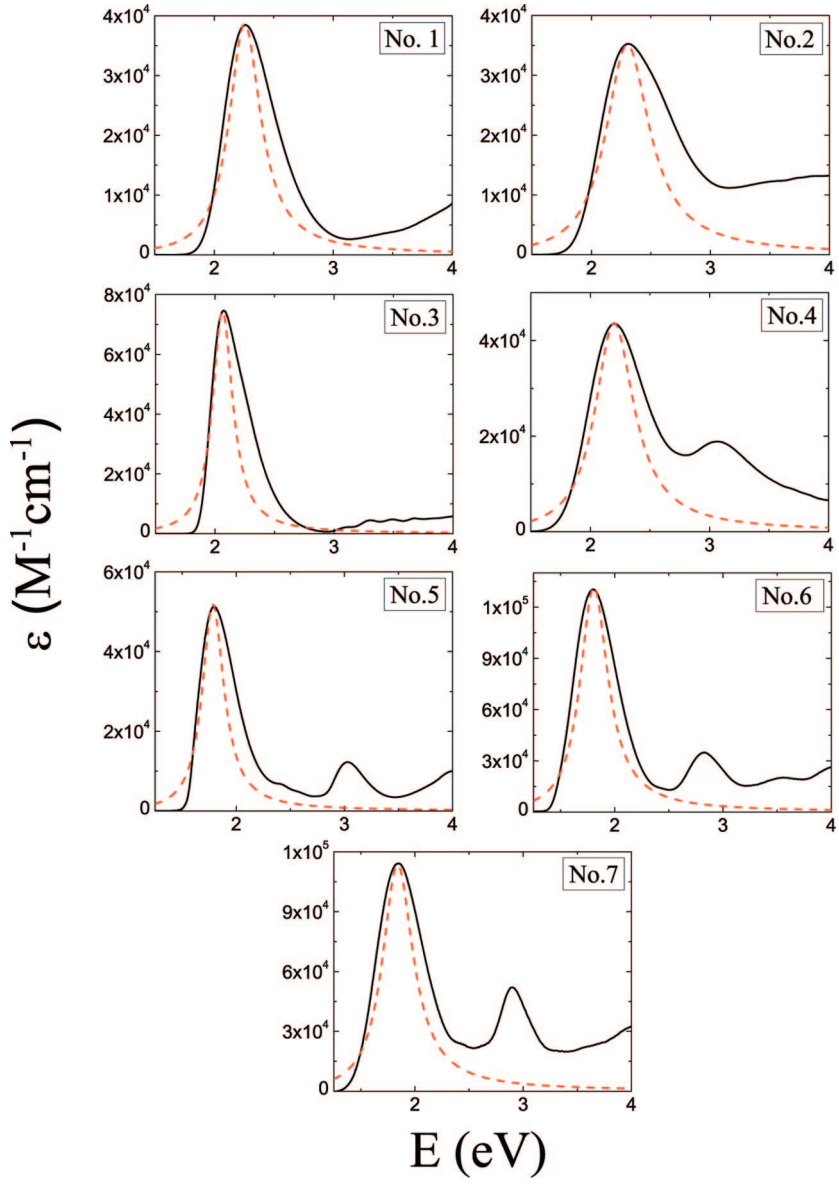

Figure 5. Molar extinction ε as a function of photon energy for the series of chromophores, as obtained from experimental linear absorption measurements on the chromophores in DMSO solution. The dashed line corresponds to the result of modeling using eq 3 with the experimental parameters obtained from the molar extinction spectra (listed in Table 1).

Table 1. Energy Differences between the First Excited State and the Ground State (E_{10}), Dressed Transition Dipole Moments ($|\mu^*_{10}|$), and Linewidths of the First Excited State (Γ) for Chromophores **1**−**7** Dissolved in DMSO[a]

molecule	E_{10} (eV)	$\|\mu^*_{10}\|$ (D)	Γ (eV)
1	2.25 ± 0.01	8.92 ± 0.05	0.162 ± 0.002
2	2.29 ± 0.01	9.92 ± 0.08	0.224 ± 0.004
3	2.06 ± 0.01	10.40 ± 0.06	0.104 ± 0.001
4	2.19 ± 0.01	10.69 ± 0.10	0.200 ± 0.004
5	1.78 ± 0.01	10.10 ± 0.05	0.123 ± 0.001
6	1.80 ± 0.01	18.13 ± 0.10	0.157 ± 0.002
7	1.83 ± 0.01	17.56 ± 0.13	0.173 ± 0.003

[a] All of the values were obtained from molar extinction spectra.

energy, as given by eq 3. The results are shown as the dashed curves in Figure 5. There is good agreement between the experimental data and the behavior predicted by the theoretical model (eq 3), confirming that our method is robust and that the characterization of experimental parameters is accurate. Therefore, we can qualitatively analyze the effects of the different conjugation paths by examining the general trends of the molar extinction spectra. All of the compounds show evidence of higher-energy resonances beyond the first peak (evidencing higher excited states that might contribute to the response), but the shapes of the extra peaks are better resolved as the degree of conjugation increases. While the number and type of secondary peaks beyond the first peak for chromophores **1**−**3** are not clearly resolved, the secondary peaks are easy to localize and characterize for chromophores **4**−**7**. This agrees qualitatively with what would be expected if indeed the oscillations in the potential function result in localization of the higher-energy eigenfunctions.

Second-Order Characterization: Hyper-Rayleigh Scattering. The first hyperpolarizabilities (β_{zzz}) of the chromophores in DMSO solution were determined by hyper-Rayleigh scattering (HRS),[33−35] which is an incoherent second-order nonlinear scattering technique; therefore, incoherent multiphoton fluorescence can contribute to the signal and result in a systematic overestimation of the first hyperpolarizability.[36] To eliminate this problem, a fluorescence-suppression scheme based on demodulation (decrease in amplitude) of the time-delayed fluorescence for high amplitude modulation (AM) frequencies was implemented. The AM frequencies were obtained as the higher harmonics of the 80 MHz repetition rate of a femtosecond titanium−sapphire laser. The output was a train of laser pulses, each ∼130 fs in duration, that were 12.5 ns apart and had a fundamental wavelength of 800 nm.[37] The method allows one to determine the presence of multiphoton fluorescence contributions to the HRS signal and correct for them by taking the high-frequency limit, where fluorescence can no longer contribute. Furthermore, when no demodulation is observed (i.e., when a constant apparent hyperpolarizability is obtained with increasing AM frequency, experimentally verified as a zero slope in units of esu/MHz), the signal is pure HRS with no multiphoton fluorescence background. An accurate average hyperpolarizability can then be obtained from the values at different AM frequencies.

Table 2. Wavelengths of Maximum Absorption (λ_{max}), Energy Differences between the Ground and Excited States (E_{10}), Experimental Values of the Dipolar First Hyperpolarizability at the Fundamental Wavelength of 800 nm ($\beta^{800\text{ nm}}_{zzz}$), and Extrapolated Off-Resonance Hyperpolarizabilities (β^{off}_{zzz})

			β_{zzz} values (10^{-30} esu)	
molecule	λ_{max} (nm)	E_{10} (eV)	$\beta^{800\text{ nm}\ a}_{zzz}$	β^{off}_{zzz}
1	551	2.25	240	110
2	540	2.29	250	110
3	602	2.06	440	240
4	567	2.19	680	340
5	695	1.78	570	280
6	691	1.80	1460	735
7	677	1.83	1510	800

[a] The experimental uncertainty in the hyperpolarizability is 10−15%.

Crystal violet in methanol was used as a reference at the fundamental wavelength of 800 nm, with $\beta^{800\text{ nm}}_{xxx} = 338 \times 10^{-30}$ esu for the hyperpolarizability tensor components.[38,39] The effects of the different symmetries (octopolar for the reference, dipolar for the chromophores) and the effective local fields at the optical frequencies were all taken into account. The dependence of the HRS signal on the concentration was confirmed to be in the linear regime for each measured solution, and the second-harmonic intensity was found to be a quadratic function of the fundamental intensity.[40] Since the HRS cell was 1 cm wide, when all of the chromophores had the same concentration during the HRS measurements, self-absorption of the signal at the second-harmonic wavelength was avoided. Standard Lorentz local-field correction factors,[41] $[(n_D^2 + 2)/3]^3$, where n_D is the refractive index of the solvent at the sodium D line, were used to determine the vacuum hyperpolarizabilities.

The dynamic hyperpolarizability and the real and imaginary parts of the linear polarizability (the refractive index and extinction coefficient, respectively) are wavelength-dependent because of the electronic resonance. To eliminate the effects of resonance enhancement, the experimental results were extrapolated to the off-resonance regime using a two-level-model approximation for the wavelength dependence of the (dipolar) first hyperpolarizability, which should be applicable to systems with a single charge-transfer band:[42]

$$\beta^{off}_{zzz} = \beta^{800\text{ nm}}_{zzz}\left[1 - \left(\frac{\lambda_{max}}{800}\right)^2\right]\left[1 - \left(\frac{\lambda_{max}}{400}\right)^2\right] \qquad (4)$$

where β^{off}_{zzz} is the extrapolated off-resonance first hyperpolarizability, $\beta^{800\text{ nm}}_{zzz}$ is the experimentally measured first hyperpolarizability at the fundamental wavelength of 800 nm, and λ_{max} is the wavelength of maximum absorption (in units of nm). The experimental values $\beta^{800\text{ nm}}_{zzz}$ and the extrapolated off-resonance values β^{off}_{zzz} for **1**−**7** are tabulated in Table 2, along with the λ_{max} values and the E_{10} values derived from them.

Analysis of the Nonlinear Response in Terms of the Quantum Limits

Although comparisons between the hyperpolarizabilities β^{off}_{zzz} of different compounds can be used to determine the factors that enhance the nonlinear response, these values do not determine the intrinsic nonlinear efficiency of a molecule. For

(29) Tripathy, K.; Pérez-Moreno, J.; Kuzyk, M. G.; Coe, B. J.; Clays, K.; Kelley, A. M. *J. Chem. Phys.* **2004**, *121*, 7932–7945.
(30) Tripathy, K.; Pérez-Moreno, J.; Kuzyk, M. G.; Coe, B. J.; Clays, K.; Kelley, A. M. *J. Chem. Phys.* **2006**, *125*, 79905.
(31) Orr, B. J.; Ward, J. F. *Mol. Phys.* **1971**, *20*, 513–526.
(32) Limpoert, E.; Stahel, W. A.; Abbt, M. *BioScience* **2001**, *51*, 341–352.
(33) Clays, K.; Persoons, A. *Phys. Rev. Lett.* **1991**, *66*, 2980–2983.
(34) Clays, K.; Persoons, A. *Rev. Sci. Instrum.* **1992**, *63*, 3285–3289.
(35) Clays, K.; Persoons, A.; De Maeyer, L. In *Modern Nonlinear Optics*; Prigogine, I., Rice, S. A., Eds.; Advances in Chemical Physics, Vol. 85; John Wiley & Sons: New York, 1994.
(36) Noordman, O. F. J.; van Hulst, N. F. *Chem. Phys. Lett.* **1996**, *253*, 145–150.
(37) Olbrechts, G.; Strobbe, R.; Clays, K.; Persoons, A. *Rev. Sci. Instrum.* **1998**, *69*, 2233–2241.
(38) Verbiest, T.; Clays, K.; Samyn, C.; Wolff, J.; Reinhoudt, D.; Persoons, A. *J. Am. Chem. Soc.* **1994**, *116*, 9320–9323.
(39) Clays, K.; Persoons, A. *Rev. Sci. Instrum.* **1994**, *65*, 2190–2194.
(40) Olbrechts, G.; Wostyn, K.; Clays, K.; Persoons, A. *Opt. Lett.* **1999**, *24*, 403–405.
(41) Kuzyk, M. G. In *Characterization Techniques and Tabulations for Organic Nonlinear Optical Materials*, 2nd ed.; Kuzyk, M. G., Dirk, C. W., Eds.; Marcel Dekker: New York, 1998; pp 111−220.
(42) Oudar, J. L.; Chemla, D. S. *J. Chem. Phys.* **1977**, *66*, 2664–2668.

example, two molecules with the same first hyperpolarizability but a very different number of delocalized π electrons contributing to the response are not intrinsically equivalent. Clearly, the molecule with fewer delocalized electrons is more efficient if the first hyperpolarizabilities are the same. A fair comparison requires that the theory quantify the nonlinear efficiency of a system in terms of fundamental physical parameters. Such a theory was developed by Kuzyk and co-workers[29,43−49] and shows that the quantum sum rules impose limits on the first and second hyperpolarizabilities.

The upper bounds depend on the number of delocalized electrons and the wavelength of maximum absorption of the system and are calculated by applying the Thomas−Kuhn sum rules to the sum-over-states (SOS) expression for the hyperpolarizability tensor obtained from perturbation theory. The Thomas−Kuhn sum rules relate the transition dipole moments μ_{mn} to the energy level separations $E_{mn} = E_m - E_n$. Using the three-level-model ansatz[48,50−52] for the off-resonant hyperpolarizability yields the following expression for $\beta_{zzz}^{\text{off-max}}$, the fundamental limit of the off-resonant first hyperpolarizability:

$$\beta_{zzz}^{\text{off-max}} = \sqrt[4]{3}\left(\frac{e\hbar}{\sqrt{m}}\right)^3 \frac{N^{3/2}}{E_{10}{}^{7/2}} \tag{5}$$

in which N is the effective number of polarizable electrons and m is the electron mass. It should be noted that the energy difference E_{10} is proportional to the reciprocal of $\lambda_{\max}$ for the ground to first excited state transition. In the off-resonance regime, the first hyperpolarizability of a molecule is optimized when the strength of the transition dipole moment to the first excited state is approximately three-fourths of the maximum sum-rule-allowed value and the energy to the second excited state becomes large compared with that to the first excited state.[29,30,43−46,48,49]

The intrinsic efficiency of a nonlinear response is given by the scale-invariant ratio between the measured first hyperpolarizability of the molecule and the quantum limit.[22] To emphasize the intrinsic (size-independent) nature of the ratio, it is called the *intrinsic hyperpolarizability*.[23] It is important to note that the intrinsic hyperpolarizability depends only on the number of delocalized electrons and two experimental quantities: the wavelength of maximum absorption and the measured first hyperpolarizability. Thus, the nonlinear efficiency of a particular system is quantified without the need to make comparisons between molecules; instead, it is an absolute quantity. The intrinsic hyperpolarizability is dimensionless and varies from 0 (when the molecule shows no second-order nonlinear response) to 1 (when the arrangement of delocalized electrons is optimal). In fact, a survey of the best molecules that had been reported through the year 2004 showed that the intrinsic hyperpolarizabilities of all of them are a factor of $10^{3/2}$ below the fundamental limit, which has become known as the *apparent limit*.[29,30,43,44] There is no explanation for the gap between the apparent and fundamental limits, although Tripathi and co-workers[29,30] have shown that the apparent limit is not of a fundamental nature and therefore is breachable.

Quantum-Limits Analysis in the Off-Resonance Regime. The resulting simplified SOS expression for the off-resonant hyperpolarizability β_{zzz}^{off} obtained using the three-level-model ansatz[50−52] can be expressed as[29,30,53]

$$\beta_{zzz}^{\text{off}}(E, X) = \beta_{zzz}^{\text{off-max}} f(E) G(X) \tag{6}$$

where $\beta_{zzz}^{\text{off-max}}$ is given by eq 5 and $f(E)$ and $G(X)$ are given by

$$f(E) = (1 - E)^{3/2}\left(E^2 + \frac{3}{2}E + 1\right) \tag{7}$$

$$G(X) = \sqrt[4]{3} X \sqrt{\frac{3}{2}(1 - X^4)} \tag{8}$$

in which we have introduced the dimensionless quantities X and E, defined as

$$X \equiv \frac{|\mu_{10}|}{|\mu_{10}^{\max}|} = \frac{|\mu_{10}|}{\sqrt{\frac{(e\hbar)^2 N}{2m}}} \tag{9}$$

$$E \equiv \frac{E_{10}}{E_{20}} \tag{10}$$

where E_{20} is the energy difference between the ground and second excited states.

Both X and E range from 0 to 1. The off-resonance first hyperpolarizability is maximal when both $f(E)$ and $G(X)$ are independently optimized. Optimization of eqs 7 and 8 yields $f_{\max} = f(0) = 1$ and $G_{\max} = G(3^{-1/4}) = 1$, which in turn gives $\beta_{zzz}^{\text{off}} f(0) G(3^{-1/4}) = \beta_{zzz}^{\text{off-max}}$. In other words, in the off-resonance regime, the molecule is optimized when the strength of its transition dipole moment is approximately three-fourths of the maximum sum-rule-allowed dipole-moment strength to the first excited state and the energy to the second excited state becomes infinitely large compared with that to the first excited state.

The fundamental-limits analysis is used in combination with experimental values to gain a deeper understanding of the nonlinear response of molecules. By means of the protocol developed by Tripathi and co-workers,[29,30] experiments can be used to determine $G(X)$ and $f(E)$ as follows. First, the values of μ_{10} and E_{10} are obtained from the UV−vis absorption spectrum (in the present work, these values are listed in Table 1). From eq 9, the value of X is calculated using μ_{10} and N, the effective number of delocalized electrons in the molecule. From the X value, $G(X)$ can be calculated using eq 8. From this set of measurements and calculations, $f(E)$ is determined by using eqs 6 and 5 and the experimental value of β_{zzz}^{off}. Finally, from $f(E)$, E can be obtained by numerical inversion.

The above procedure, which determines the values for X and E, allows us to analyze the nonlinear response of a molecule in terms of the normalized transition dipole moment parameter X and the energy parameter E. It should be pointed out that while in principle the fundamental-limits analysis should work better when the nonlinear response of a system is due to the contribution of only a few excited states, in a system with many

(43) Kuzyk, M. G. *Circuits and Devices* **2003**, *19*, 8–17.
(44) Kuzyk, M. G. *Opt. Photonics News* **2003**, *14*, 26.
(45) Kuzyk, M. G. *Phys. Rev. Lett.* **2000**, *85*, 1218–1221.
(46) Kuzyk, M. G. *Opt. Lett.* **2000**, *25*, 1183–1185.
(47) Kuzyk, M. G. *IEEE J. Sel. Top. Quantum Electron.* **2001**, *7*, 774–780.
(48) Kuzyk, M. G. *Phys. Rev. Lett.* **2003**, *90*, 39902.
(49) Kuzyk, M. G. *Opt. Lett.* **2003**, *28*, 135.
(50) Kuzyk, M. G. *Phys. Rev. A* **2005**, *72*, 053819.
(51) Kuzyk, M. G.; Watkins, D. S. *J. Chem. Phys.* **2006**, *124*, 244104.
(52) Kuzyk, M. C.; Kuzyk, M. G. *J. Opt. Soc. Am. B* **2008**, *25*, 103–110.
(53) Pérez-Moreno, J.; Asselberghs, I.; Zhao, Y.; Song, K.; Nakanishi, H.; Okada, S.; Nogi, K.; Kim, O.-K.; Je, J.; Mátrai, J.; Maeyer, M. D.; Kuzyk, M. G.; Clays, K. *J. Chem. Phys.* **2007**, *126*, 074705.

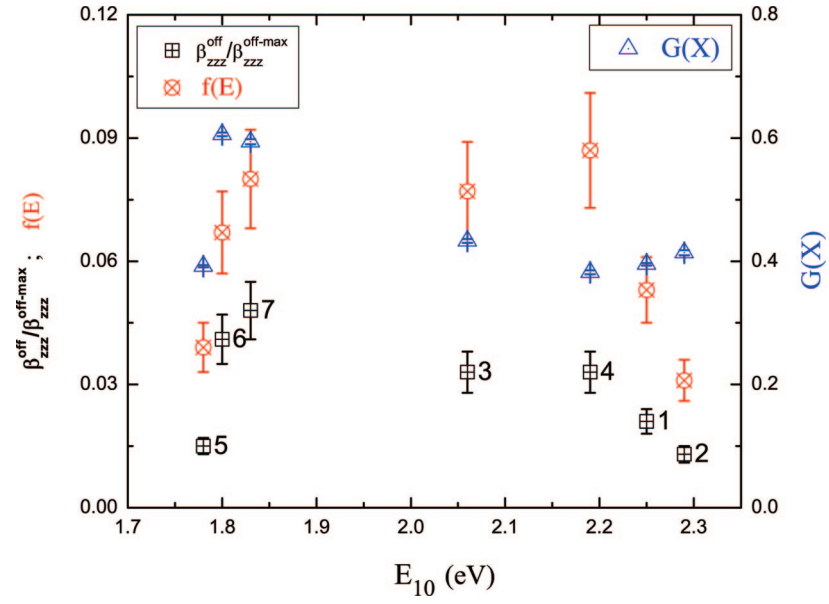

Figure 6. Values of $G(X)$, $f(E)$, and the intrinsic hyperpolarizability $\beta_{zzz}^{off}/\beta_{zzz}^{off\text{-}max}$ for the collection of molecules as functions of photon energy.

Table 3. Values of E_{10}, X, $G(X)$, $\beta_{zzz}^{off}/\beta_{zzz}^{off\text{-}max}$, and $f(E)$ Obtained from an Analysis of the Experimental Values for **1**−**7**, Along with Extrapolated Values of E and E_{20} Obtained from the Values of $f(E)$ Using Equation 7

molecule	E_{10} (eV)	X	$G(X)$	$\beta_{zzz}^{off}/\beta_{zzz}^{off\text{-}max}$	$f(E)$	E	E_{20} (eV)
1	2.25	0.245 ± 0.001	0.395 ± 0.002	0.021 ± 0.003	0.053 ± 0.008	0.936	2.40
2	2.29	0.257 ± 0.002	0.414 ± 0.004	0.013 ± 0.002	0.031 ± 0.005	0.956	2.40
3	2.06	0.269 ± 0.002	0.433 ± 0.003	0.033 ± 0.005	0.077 ± 0.012	0.917	2.25
4	2.19	0.238 ± 0.002	0.382 ± 0.003	0.033 ± 0.005	0.087 ± 0.014	0.909	2.41
5	1.78	0.243 ± 0.001	0.392 ± 0.002	0.015 ± 0.002	0.039 ± 0.006	0.948	1.88
6	1.80	0.380 ± 0.002	0.606 ± 0.003	0.041 ± 0.006	0.067 ± 0.010	0.924	1.95
7	1.83	0.372 ± 0.003	0.594 ± 0.004	0.048 ± 0.007	0.080 ± 0.012	0.914	2.00

levels, the energy function $f(E)$ and the normalized energy E can be visualized as a proxy for the energy-level spacing of the molecule. When $f(E) = 1$, the energies are arranged in an optimal way, while when $f(E)$ is small, the energy-level spacing causes β_{zzz}^{off} to vanish.

The results of the quantum-limits analysis in the off-resonance regime are listed in Table 3. Figure 6 summarizes the results of the analysis by plotting $G(X)$, $f(E)$, and the intrinsic hyperpolarizability $\beta_{zzz}^{off}/\beta_{zzz}^{off\text{-}max}$. For comparison, we will first review the results of our previous analysis of systems with high nonlinear efficiencies that followed the traditional paradigm for the conjugated spacer (a polyene bridge with a sequence of alternating double and single carbon−carbon bonds).[29,30] The study showed that a suboptimal energy distribution is responsible for the low efficiency of typical molecules, which have many closely spaced excited-state energies that dilute the nonlinear-transition strength from the low-lying states.[29,30] When we compare the best values of $G(X)$ and $f(E)$ *independently* for the series of traditional structures[29,30] and the results from this study (Table 3), we find similar best values [~0.5 for $G(X)$ and 0.07 for $f(E)$] with no correlation between the two functions for molecules that follow the traditional design.

When we consider molecules with modulated conjugation, we observe the trend that an increase in the degree of modulation is accompanied by a simultaneous increase in $G(X)$ and $f(E)$. This is an interesting result, particularly in view of a previous study where we tried to enhance the nonlinear response by changing the molecular environment using an amylose jacket.[53] While the strategy worked globally, that study indicated that there was a tradeoff: inclusion of a molecule resulted in better energy-level spacing, which overcame the resulting decrease in transition moments between states. To our knowledge, our present work is the first report of an enhancement strategy that works by optimizing both the transition moments and the energy spacing *simultaneously*.

The poor performance of chromophore **5** is most likely due to a break in the conjugation path. Steric hindrance caused by interactions of the chlorine with the carbonyl or phenyl groups should induce a twist in the bond between the thiazine and the isoxazylene and therefore a break in the conjugation path. In the same manner, steric hindrance should induce a twist in the conjugation path for chromophore **6** (which is isoelectronic to chromophore **7**).

It is interesting to compare the performance of our chromophore **7** with a well-known chromophore in second-order nonlinear optics, the FTC chromophore (2-dicyanomethylen-3-cyano-4-{2-[(*E*)-(4-*N*,*N*-bis(2-acetoxyethyl)amino)phenylene-(3,4-dibutyl)thien-5]-(*E*)-vinyl}-5,5-dimethyl-2,5-dihydrofuran).[17,54] FTC is structurally similar to chromophore **7** (see Figure 7) but has a lower degree of modulated conjugation (one of the repeated C═C double bonds along the path in FTC is substituted by a N═N double bond in chromophore **7**).

From the higher degree of modulated conjugation of chromophore **7**, we should expect a better nonlinear performance. Indeed, the HRS characterization of FTC in chloroform ($\beta_{zzz}^{off} = 635 \times 10^{-30}$ esu, $\lambda_{max} = 650$ nm), yields a slightly lower intrinsic hyperpolarizability ($\beta_{zzz}^{off}/\beta_{zzz}^{off\text{-}max} = 0.043$). Thus, the quantum-limits analysis confirms that for FTC, "*the molecular hyperpolarizability of the chromophore is exceptional*" with "*dramatically improved*

(54) Kinnibrugh, T.; Bhattacharjee, S.; Sullivan, P.; Isborn, C.; Robinson, B. H.; Eichinger, B. E. *J. Phys. Chem. B* **2006**, *110*, 13512–13522.

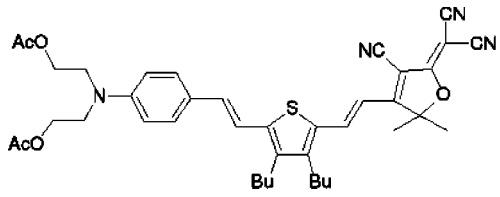

Figure 7. Chemical structure of the FTC chromophore.[17]

optical nonlinearity".[17] Robinson et al.[17] performed computer simulations using AM1 calculations, which indicated that the conjugated path is almost planar, maximizing the delocalized π-orbital overlap. We believe that part of the exceptional optical nonlinearity of FTC is due to the modulated nature of the bridge, which also explains why chromophore **7** (with a slightly higher degree of modulated conjugation along the path) performs better than FTC.

Recently, Kinnibrugh et al.[54] performed quantum-mechanical studies of the FTC chromophore. They concluded that all of the different low-energy rotamers contribute to the response, and they predicted a statistical-mechanical-average off-resonance hyperpolarizability (in vacuum) of $\beta_{zzz}^{\text{off}} = 584 \times 10^{-30}$ esu at $T = 289.16$ K and a factor enhancement of $\sim$2.5$-$4.5 due to the reaction field. The vacuum statistical average is in good agreement with the value reported by Robinson et al., which most likely means that rotamers with different energies contribute to the first hyperpolarizability of chromophore **7**. More importantly, they concluded that interchanging the locations of the thiophene and *p*-phenylene groups in the conjugated backbone joining the donor and acceptor groups gives a relatively small change in the hyperpolarizability. This could suggest that when searching for an optimal structure, we should focus on inducing uneven oscillations in the potential rather than on the specific order of such oscillations, which is in agreement with the numerical results by Zhou et al.[21]

Also, Schmidt et al.[55] performed quantum calculations to study the role of the TFC group (2-dicyanomethylidene-3-cyano-4,5,5-trimethyl-2,5-dihydrofuran), the acceptor group in the FTC chromophore. They performed SOS calculations to investigate the effect of replacing the oxygen atom of the furan ring in the TCF group. The study showed that there is a correlation between the inductive electron-withdrawing character of the substituted group (X) and the first hyperpolarizability β_{zzz}^{off} (with β_{zzz}^{off} being further increased or decreased when X has π-accepting or π-donating character, respectively). Interestingly, their analysis of the fully converged results for β_{zzz}^{off} (including the contributions of the 30 highest occupied states and the 30 lowest unoccupied states) showed that effective use of a three-level model (i.e., inclusion of all the contributions to β_{zzz}^{off} from the ground and first two dominant excited states) reproduced the trends of the fully converged results for all modeled molecules (a total of 30 structures). These results seem to provide further evidence for the validity of our analysis, especially when we look at the more highly modulated compounds, where the linear absorption indicates the existence of two dominant excited states. This supports the three-level ansatz.

Analysis of the On-Resonance Response. It is important to note that the computation of the energy function $f(E)$ is based on the experimental results and the fact that with three levels it is possible to factorize the first hyperpolarizability into one term that depends only on transition dipole moments, $G(X)$, and another term that only depends on energy. Therefore, comparison of different energy functions works as a proxy for the energy-level spacing of the molecules, especially when the values of $G(X)$ are on the order of unity, which indicates that indeed the contribution of the first two excited levels dominates the response. In this sense, our conclusion that this new enhancement strategy optimizes both the transition moments and the energy spacing is general. Furthermore, even in cases where the extrapolation to the off-resonance regime might not be correctly deduced from eq 4, the effects are minimal and should not affect our conclusions, since the extrapolation factor is similar for all of the chromophores (as they all have similar values of $\lambda_{\max}$) and amounts to a similar degree of scaling of the intrinsic hyperpolarizability. This scaling has no effect on the relative performance of the molecules, so our conclusion that the enhancement strategy works and optimizes both the transition overlap and the energy spacing is minimally affected by this approximation.

We used the value of $f(E)$ to obtain the energy of the second excited state, E_{20}, as shown in Table 3. These results can be compared with the molar extinction spectra shown in Figure 5. For molecules **4**, **5**, **6** and **7** (the ones where the secondary peaks are distinguishable), the predicted second excited state energies fall short of the positions of the secondary peaks by $\sim$1 eV. This should be interpreted in the context of using three levels as a proxy for optimal response: the effective second excited state, E_{20}, accounts for the contributions of all of the higher excited states.

To refine our approach, we again assume three dominant states and apply the sum rules to calculate the dispersion of β, allowing us to model resonance enhancement of the nonlinear optical response without the need to extrapolate to the off-resonance regime.[56] Since the photon energy of the second-harmonic signal is $\sim$3.1 eV (400 nm), it is clear from the molar extinction spectra shown in Figure 5 that we should expect a resonant contribution from the second excited state, especially for molecules **4**, **5**, **6**, and **7**, where the secondary peaks are in the vicinity of 3.1 eV. With resonance enhancement from the second excited level, the response of the first hyperpolarizability should be dominated by the first three levels. This is in contrast with the off-resonance analysis, where in principle, the contributions of higher states are more strongly weighted in the calculation of the zero-frequency limit of the hyperpolarizability. Thus, while the off-resonance analysis gives us E_{20} as a proxy for the higher levels, an on-resonance analysis should provide a more realistic value of the second-excited-state properties.

The three-level ansatz,[52] when applied to the dispersion of the first hyperpolarizability, yields:[22,50]

$$\beta_{zzz}(\hbar\omega_1, \hbar\omega_2) = G(X)\beta_{zzz}^{\text{off-max}} F(\hbar\omega_1, \hbar\omega_2, E_{10}, E_{20}, \Gamma_{10}, \Gamma_{20}) \tag{11}$$

where $\hbar\omega_1$ and $\hbar\omega_2$ are the photon energies, Γ_{10} and Γ_{20} are the state linewidths (inverse radiative lifetimes) of the first and second excited states, respectively, and the on-resonance energy function F is defined by[56]

$$F(\hbar\omega_1, \hbar\omega_2, E_{10}, E_{20}, \Gamma_{10}, \Gamma_{20}) = \frac{1}{6}E_{10}\sqrt{\frac{1}{E_{20}(E_{20} - E_{10})}} \times \left\{P_{\hbar\omega_1,\hbar\omega_2}\left[D_{21} - D_{22}\left(2\frac{E_{10}}{E_{20}} - 1\right) + D_{12} - D_{11}\left(2\frac{E_{20}}{E_{10}} - 1\right)\right]\right\} \tag{12}$$

In eq 12, the permutation operator $P_{\hbar\omega_1,\hbar\omega_2}$ operates on the expression in square brackets, generating additional terms in which

(55) Schmidt, K.; Barlow, S.; Leclercq, A.; Zojer, E.; Jan, S.-H.; Marder, S. R.; Jen, A. K.-Y.; Bredás, J. L. *J. Mater. Chem.* **2007**, *27*, 2944–2949.

(56) Kuzyk, M. G. *J. Chem. Phys.* **2006**, *125*, 154108.

Table 4. Energy Differences between the First Excited State and Ground State (E_{10}), Linewidths of the First Excited State (Γ_{10}), and the Ratios $\beta_{zzz}^{800\ nm}/[G(X)\beta_{zzz}^{off\text{-}max}]$, Along with Values of E_{20} Obtained from Equation 12 and the Data with $\Gamma_{20} = \Gamma_{10}/2$ and (When Available) E_{20} Values from the Molar Extinction Spectra

				E_{20} (eV)	
molecule	E_{10} (eV)	Γ_{10} (eV)	$\beta_{zzz}^{800\ nm}/[G(X)\beta_{zzz}^{off\text{-}max}]$	from eq 12	from spectrum
1	2.25	0.162 ± 0.002	0.11 ± 0.02	3.11	—
2	2.29	0.224 ± 0.004	0.07 ± 0.010	3.12	—
3	2.06	0.104 ± 0.001	0.14 ± 0.02	3.11	-?-
4	2.19	0.200 ± 0.004	0.17 ± 0.013	3.12	3.06
5	1.78	0.123 ± 0.001	0.077 ± 0.013	3.12	3.03
6	1.80	0.153 ± 0.002	0.13 ± 0.02	3.14	2.83
7	1.83	0.173 ± 0.003	0.15 ± 0.02	3.15	2.90

the quantities $\hbar\omega_1$ and $\hbar\omega_2$ have been permuted (interchanged). The only quantities in the bracketed expression that depend on $\hbar\omega_1$ and $\hbar\omega_2$ are the dispersion functions D_{nm} ($n, m = 1, 2$). D_{nm} is a function of the quantities E_{n0}, E_{m0}, Γ_{n0}, Γ_{m0}, $\hbar\omega_1$, and $\hbar\omega_2$ and is given by the first three terms in eq 13 below. Thus, the effect of $P_{\hbar\omega_1,\hbar\omega_2}$ in eq 12 can be expressed in terms of the relation

$$P_{\hbar\omega_1,\hbar\omega_2}(D_{nm}) = \frac{1}{2}\left\{\frac{1}{(E_{n0} - i\Gamma_{n0} - \hbar\omega_1 - \hbar\omega_2)(E_{m0} - i\Gamma_{m0} - \hbar\omega_1)} + \frac{1}{(E_{n0} + i\Gamma_{n0} + \hbar\omega_2)(E_{m0} - i\Gamma_{m0} - \hbar\omega_1)} + \frac{1}{(E_{n0} + i\Gamma_{n0} + \hbar\omega_2)(E_{m0} + i\Gamma_{m0} + \hbar\omega_1 + \hbar\omega_2)} + \text{three additional terms identical to the above except that } \hbar\omega_1 \text{ and } \hbar\omega_2 \text{ are interchanged}\right\} \quad (13)$$

We tested the consistency of our three-level approach by using eq 11 to calculate the real part of $F(\hbar\omega_1, \hbar\omega_2, E_{10}, E_{20}, \Gamma_{10}, \Gamma_{20})$ from the HRS results at a fundamental wavelength of 800 nm directly from the ratio

$$\frac{\beta_{zzz}^{800\ nm}}{G(X)\beta_{zzz}^{off\text{-}max}} \quad (14)$$

and then using eq 12 to solve for E_{20}. We emphasize that without further measurements, we cannot determine all of the parameters needed to model the first hyperpolarizability, even with only three levels. While the values of μ_{20} and Γ_{20} can be determined from the second peak in the molar extinction spectrum, the three-level model also requires the value of μ_{21}, which is not directly measurable. However, if we add the extra conditions imposed by the sum rules, the three-level model for the first hyperpolarizability is simplified so that it can be modeled using eq 11.[56] Real molecules whose hyperpolarizabilities are far from the quantum limits may have more than three contributing states, so we tested the validity of our approach by comparing the values of E_{20} predicted using the sum rules in a three-level system with the measured second peaks in the molar extinction spectra. The results are shown in Table 4. The predicted values of E_{20} are in good agreement with the positions of the secondary peaks (with a deviation of less than 10% between the two values in each case) and are much better than the off-resonant predictions in Table 3. This good agreement is an indicator of the robustness of our method, but we should be cautious about drawing specific conclusions. Proper modeling of the nonlinear response near resonance is sensitive to parameter values, and a more careful analysis is beyond the scope of the present work.

Conclusions

We propose a strategy for the optimization of the molecular nonlinear optical response that is based on modulated conjugation of the spacer in linear molecules. A series of chromophores with different types of modulated conjugated paths were synthesized, and the linear and nonlinear optical properties of the compounds were characterized through hyper-Rayleigh scattering. Our experimental results confirm the numerical simulations, which suggest that modulated conjugation is a viable strategy for enhancing the intrinsic hyperpolarizability of organic compounds.[21] Unlike other proposed strategies that rely on perfect "tuning" of the potential energy function (such as the clipped harmonic oscillator potential),[29,30] this new strategy suggests the general principle of modulating the conjugated path by using a variety of aromatic moieties in series between the donor and the acceptor. Therefore, it should be straightforward to apply our paradigm to the design and synthesis of molecular structures with enhanced hyperpolarizability.

A systematic quantum-limit analysis of linear absorption and HRS for a series of molecules suggests that modulation of the potential energy function results in an increase in the intrinsic hyperpolarizability by concentrating the response to only a few contributing states. The quantum-limit analysis shows that this optimization strategy works by *simultaneously* optimizing the transition dipole moments and the energy spacing in a molecule.

We have applied the theory of the dispersion of the dipole-free SOS expression of the hyperpolarizability using the three-level ansatz in order to interpret the near-resonance HRS measurements. The results are consistent with our assumptions and show that we can use the quantum-limit analysis to increase our understanding of the nonlinear response by extracting the maximum amount of information from the experimental data using a minimum number of general assumptions.

In summary, our work proposes conjugation of modulation as a new paradigm for making molecules with enhanced intrinsic hyperpolarizability. A theoretical analysis of our method shows that this approach simultaneously optimizes both the oscillator strength and the energy-level spacing. Furthermore, the sum-rule-based theory is found to approximate the energy of the second excited state, which validates the theory and provides a new approach for describing the dispersion of the nonlinear optical response with a minimal number of parameters, making it possible to experimentally parametrize the nonlinear response. As such, our work may both lead to a deeper understanding of the dispersion of the hyperpolarizability and provide chemists with a new synthetic route for making more efficient nonlinear optical molecules.

Acknowledgment. J.P.-M. acknowledges the Fund for Scientific Research Flanders (FWO). M.G.K. thanks the National Science Foundation (Grant ECCS-0756936) and Wright Patterson Air Force Base for generous support of this work.

Supporting Information Available: Complete ref 17. This material is available free of charge via the Internet at http://pubs.acs.org.

JA807394F